

Supporting Information

Pressure effects on both fluorescent emission and charge transport properties of organic semiconductors: A computational study

Yi Zeng^a, Wen Shi^b, Qian Peng,^c Yingli Niu^d, Zhiying Ma^e, Xiaoyan Zheng^{a*}

^aBeijing Key Laboratory of Photoelectronic/Electrophotonic Conversion Materials, Key Laboratory of Cluster Science of Ministry of Education, School of Chemistry and Chemical Engineering, Beijing Institute of Technology, 100081 Beijing, China. E-mail: xiaoyanzheng@bit.edu.cn

^bSchool of Chemistry, Sun Yat-sen University, Guangzhou, 510006, China.

^cKey Laboratory of Organic Solids, Beijing National Laboratory for Molecular Science (BNLMS), Institute of Chemistry, Chinese Academy of Sciences, Beijing 100190, China.

^dChina.School of Science, Beijing Jiaotong University, Beijing 100044, China.

^eEngineering Research Center for Nanomaterials, Henan University, Kaifeng 475004, China.

List of Contents

I. Computational details

1. Hole mobility calculations.

II. Supplementary Figures S1-S6

Fig. S1 Schematic representation of the charge hopping pathways from molecule A to its neighbors with probabilities p_1, p_2, \dots , and p_N .

Fig. S2 Chemical Structures of COTh. The key structural parameters and the index of every atom were labeled, respectively.

Fig. S3 Electron density contours of the HOMO and LUMO of COTh at 4.86 GPa.

Fig. S4 The energy level of HOMO and LUMO at S_0 and S_1 , respectively.

Fig. S5 The calculated λ_{gs} versus the normal-mode frequencies of the COTh aggregates under different pressure and diagrammatic illustration of selected normal modes with large λ_{gs} at 0 GPa.

Fig. S6 The contributions to the λ_{gs} from bond length (λ_{bond}), bond angle (λ_{angle}) and dihedral angle ($\lambda_{dihedral}$) under different pressure.

III. Supplementary Tables S1-S12

Table S1. The lattice parameters ($a, b, c, \alpha, \beta, \gamma$), density and volume of unit cell of COTh crystal under different external pressure.

Table S2. The calculated vertical excitation energy (ΔE_{vert}), wavelength and oscillator strength (f) of COTh crystal based on the QM/MM models at S_0 and S_1 using several different functionals with basis set 6-31G(d,p), respectively.

Table S3. The calculated elastic constants of lattice parameters a, b, c for the COTh crystal.

Table S4. The intermolecular distance (Å) between the centroid COTh and its neighbors within 12 Å.

Table S5. Selected bond length (Å), bond angles (degree) and dihedral angles (degree) of COTh crystal at the S_0 (S_1) minimum and the modifications $\Delta|S_0 - S_1|$ between the two states at different pressure (GPa).

Table S6. The calculated vertical excitation energy (ΔE_{vert}), oscillator strength (f), adiabatic excitation energy (ΔE_{ad}) and the transition orbital assignment for S_1 of COTh molecules at crystal state under different pressure.

Table S7. The calculated spin-orbit coupling constants between S_1 and triplet excited states for COTh crystals at 0 GPa and 4.86 GPa.

Table S8. The calculated k_r, k_{ic}, k_{eet} and fluorescence quantum efficiency Φ_F for the COTh aggregates under different pressure.

Table S9. The calculated $\lambda_{gs}, \lambda_{es}$ and λ_{total} of COTh in aggregates at different pressures.

Table S10. The maximum J_{max} among different dimers and spectral overlap I under different pressure for COTh crystals.

Table S11. The transfer integral V (meV) along different pathways under different pressure.

Table S12. The calculated charge reorganization energy λ_{charge} using normal mode analysis (NM) and adiabatic potential energy surface method (AP) at different pressure.

I. Computational details

1. Hole mobility calculations.

The hoping model assumes that the carrier is localized at one position in the solid and jumps from one position to another by a series of incoherent jumps. Full quantum charge transfer rate is used in hoping models:¹

$$k_{i \rightarrow f} = \frac{|V|^2}{\hbar^2} \int_{-\infty}^{\infty} dt \exp \left\{ - \sum_j S_j [(2\bar{n}_j + 1) - \bar{n}_j e^{-i\omega_j t} - (\bar{n}_j + 1)e^{i\omega_j t}] \right\} \quad (S1)$$

$$\bar{n}_j = \frac{1}{\left(e^{\frac{\hbar\omega_j}{k_B T}} - 1 \right)} \quad (S2)$$

where $k_{i \rightarrow f}$ is the rate of charge transfer between two adjacent molecules i and f , \hbar is the Plank constant and S_j measures the electron-phonon coupling strength between the carrier onsite energy and the j th intramolecular vibration mode, V is the transfer integral, \bar{n}_j is the occupation number for the j th phonon mode with vibrational frequency ω_j .

The reorganization energy is mainly the change of energy caused by geometric relaxation during charge transfer, including external reorganization energy and internal reorganization energy. The external reorganization energy is caused by the interaction of the surrounding solvent molecules, and is related to the dielectric constant of the solvent. Compared with the internal reorganization energy, it is usually negligible. Internal reorganization energy comes from the change of molecular configuration before and after charge transfer between adjacent molecules. The methods for calculating internal recombination energy include adiabatic potential energy surface method^{2, 3} and normal mode analysis method^{4, 5}. In the adiabatic potential energy surface method, the calculation expression is as follows:

$$\lambda = [E_{\pm}(Q_N) - E_{\pm}(Q_{\pm})] + [E_N(Q_{\pm}) - E_N(Q_N)] \quad (S3)$$

Where $E_{\pm}(Q_{\pm})$ and $E_N(Q_N)$ is the total energy of the optimized ionic species and neutral molecule, $E_{\pm}(Q_N)$ and $E_N(Q_{\pm})$ represent the energies of the ionic and neutral species in the geometries of the neutral and ionic species, respectively.

Normal mode analysis assigns recombination energy to each vibration pattern. Its expression is:

$$\lambda = \sum \lambda_i = \sum \frac{k_i}{2} \Delta Q_i = \sum \hbar \omega s_i \quad (S4)$$

Where ΔQ_i represents the displacement along normal mode i between the equilibrium geometries of the neutral and charged molecules, k_i and ω_j are the corresponding force constants and vibrational frequencies, s_i denotes the Huang-Rhys factor measuring charge-phonon coupling strength.

Transfer integrals describe the coupling of electrons before and after charge transfer. It depends on the position and shape of the orbitals between the neighboring molecules. It could be obtained from the site-energy overlap correction method and can be written as:⁶

$$V_{mn} = \frac{V_{mn}^0 - \frac{1}{2}(e_m + e_N)O_{mn}}{1 - O_m^2} \quad (\text{S5})$$

$$e_m = \langle \Phi_m | H | \Phi_m \rangle \quad (\text{S6})$$

$$V_{mn}^0 = \langle \Phi_m | F | \Phi_n \rangle \quad (\text{S7})$$

$$O_{mn} = \langle \Phi_m | O | \Phi_n \rangle \quad (\text{S8})$$

Where Φ_m, Φ_n represent the HOMOs or LUMOs of the neighboring molecules m and n . H and O are the dimer Hamiltonian and the overlap matrices, respectively. The B3P86/6-31G** method is chosen for the calculation of transfer integrals by Gaussian program.

After the reorganization energy and transfer integral are obtained, the mobility of hopping μ , can be evaluated from the Einstein relation.

$$\mu = \frac{e}{k_B T} D \quad (\text{S9})$$

where e is the electronic charge and D is the diffusion coefficient, which is related to the charge transfer rate k as summing over all possible hopping ways. The random walk, which is a typical kind of Monte Carlo simulation was performed to obtain the diffusion coefficient. In detail, an arbitrary molecular site in the bulk system is initially chosen as the starting position for the charge. The charge then has a probability of p_i to hop to the i -th neighbor (see Figure R3). In practice, in order to determine the next site of the charge in a statistical sense, a random number ξ uniformly distributed between 0 and 1 is generated. If $\sum_{i=1}^{b-1} p_i < \xi < \sum_{i=1}^b p_i$, the charge hops to the b -th neighbor with a hopping time $1/k_b$, which assumes no correlation between the hopping events along different pathways. The simulation continues until the diffusion distance exceeds the lattice constant by at least 2–3 orders of magnitude. This process is repeated for thousands of times and averaged to get a linear relationship between the mean-square displacement (MSD) and the simulation time.

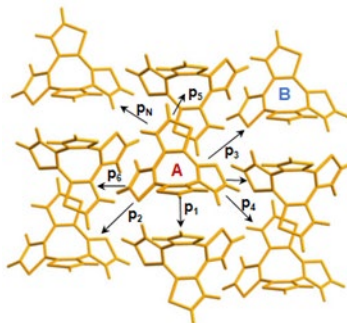


Fig. S1 Schematic representation of the charge hopping pathways from molecule A to its neighbors with probabilities p_1, p_2, \dots , and p_N .

The diffusion coefficient can be approximately evaluated as:

$$D = \frac{1}{2n} \frac{dMSD}{dt} \quad (S10)$$

where n is the dimensionality (usually n=3) of the system under investigation.

II. Supplementary Figures S2-S6

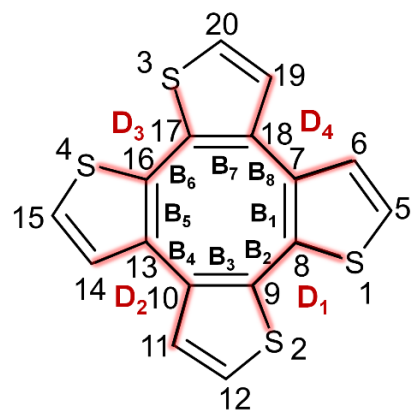


Fig. S2 Chemical Structures of COTh. The key structural parameters and the index of every atom were labeled, respectively.

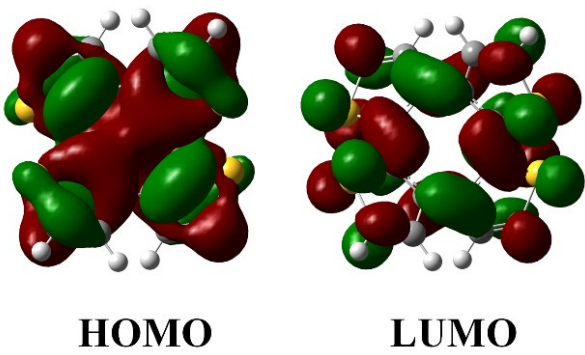


Fig. S3 Electron density contours of the HOMO and LUMO of COTh at 4.86 GPa.

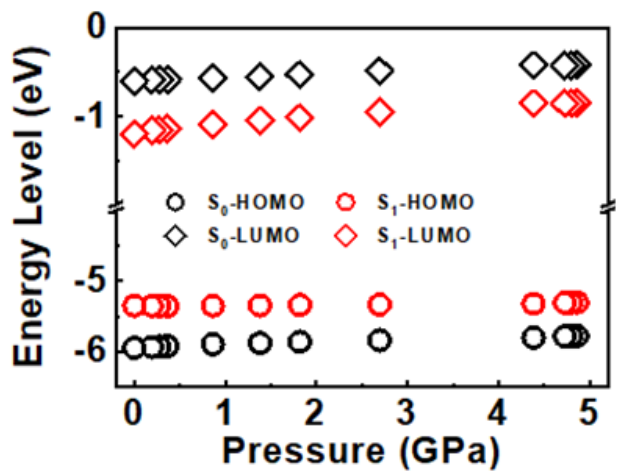


Fig. S4 The energy level of HOMO and LUMO at S_0 and S_1 , respectively.

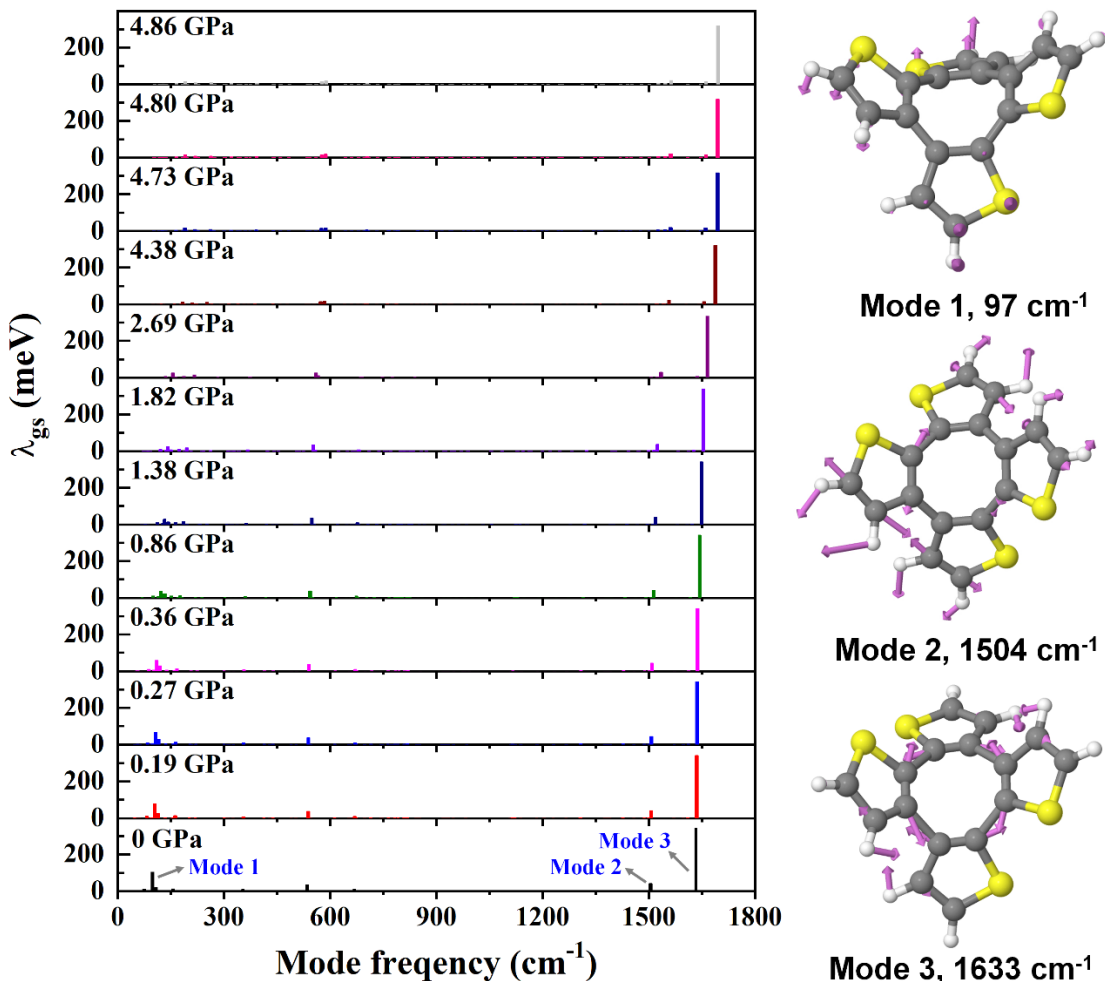


Fig. S5 The calculated λ_{gs} versus the normal-mode frequencies of the COTh aggregates under different pressure and diagrammatic illustration of selected normal modes with large λ_{gs} at 0 GPa.

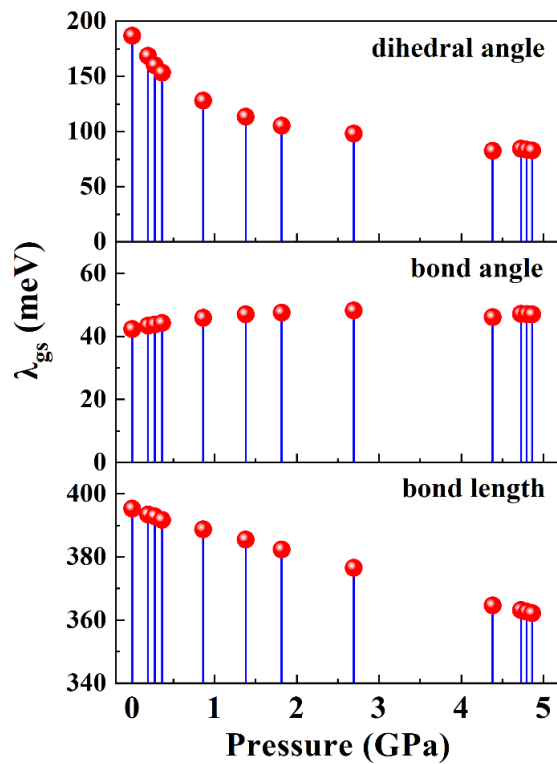


Fig. S6 The contributions to the λ_{gs} from bond length (λ_{bond}), bond angle (λ_{angle}) and dihedral angle ($\lambda_{\text{dihedral}}$) under different pressure.

III. Supplementary Tables S1-S11

Table S1. The lattice parameters (a , b , c , α , β , γ), density and volume of unit cell of COTh crystal under different external pressure.

Pressure (GPa)	Lattice parameters					Density (g/cm ⁻³)	Volume (Å ³)
	a (Å)	b (Å)	c (Å)	α (°)	β (°)		
0	9.56150	7.30270	10.33760	90.00000	103.91600	90.00000	1.56
0.19	9.50542	7.23990	10.27764	90.00000	104.04395	90.00000	1.59
0.27	9.51692	7.21582	10.22038	89.99999	103.99799	90.00000	1.60
0.36	9.49290	7.18239	10.20249	90.00001	104.09165	90.00001	1.62
0.86	9.42262	7.07097	10.10359	90.00000	104.45564	90.00001	1.67
1.38	9.34901	6.99414	10.01769	89.99999	104.56544	89.99999	1.72
1.82	9.29158	6.93575	9.95332	89.99999	104.65126	89.99999	1.76
2.69	9.19096	6.84787	9.8313	89.99999	104.69466	90.00001	1.82
4.38	9.04348	6.71362	9.65295	89.99982	104.80173	89.99992	1.92
4.73	9.08378	6.63892	9.62959	90.00035	105.17818	90.00008	1.95
4.80	9.07768	6.63421	9.62642	90.00003	105.19045	89.99998	1.95
4.86	9.07329	6.63085	9.62177	90.00031	105.20629	90.00026	1.95
							558.613

Table S2. The calculated vertical excitation energy (ΔE_{vert}), and oscillator strength (f) of COTh crystal based on the QM/MM models at S_0 and S_1 using several different functionals with basis set 6-31G(d,p), respectively.

	Absorption (S_0)		Emission (S_1)	
	ΔE_{vert}	f	ΔE_{vert}	f
Exper. ⁷			2.38 eV / 520 nm	
B3LYP	3.21 eV / 386 nm	0.0075	2.17 eV / 571 nm	0.0037
M06	3.26 eV / 381 nm	0.0080	2.20 eV / 562 nm	0.0036
BMK	3.53 eV / 351 nm	0.0093	2.31 eV / 536 nm	0.0038
BHandHLYP	3.80 eV / 326 nm	0.0115	2.43 eV / 509 nm	0.0040
M062X	3.76 eV / 330 nm	0.009	2.46 eV / 504 nm	0.0033
M052X	3.81 eV / 326 nm	0.0089	2.49 eV / 498 nm	0.0033
CAM-B3LYP	3.76 eV / 330 nm	0.0105	2.45 eV / 505 nm	0.0038
ω B97XD	3.80 eV / 327 nm	0.011	2.50 eV / 496 nm	0.0038
LC- ω HPBE	4.21 eV / 295 nm	0.0126	2.77 eV / 447 nm	0.0038

Table S3. The calculated elastic constants of lattice parameters a , b , c for the COTh crystal.

Elastic constant (GPa)	
a	36.78082
b	27.66738
b	29.32226

To calculate the elastic constant C_{ii} , we stretched the unit cell of along the a -, b -, and c -directions, respectively, by $\pm 0.5\%$, $\pm 1.0\%$, $\pm 1.5\%$, and $\pm 2.0\%$, and calculate the total energy change due to the unit-cell deformation. The elastic constant C_{ii} can be obtained by fitting the total energy E with respect to the dilation $\Delta l/l_0$, using the formula:

$$\frac{E - E_0}{V_0} = C_{ii} \frac{(\Delta l/l_0)^2}{2}$$

Here, V_0 and E_0 are, respectively, the volume and total energy of the unit cell at equilibrium. Δl is the change of lattice constant along the direction ii ($i = a, b, c$), and l_0 is its value at equilibrium. The elastic constants were calculated through first-principles calculations in Vienna Ab initio Simulation Package.

Table S4. The intermolecular distance (\AA) between the centroid COTh and its neighbors within 12 \AA .

Pressure (GPa)	1,1'	2,2'	3,3'	4,4'	5,5'	6,6'	7,7'
0	7.11	9.39	7.30	10.34	9.56	7.27	7.92
0.19	7.06	9.34	7.24	10.28	9.51	7.21	7.87
0.27	7.07	9.34	7.22	10.22	9.52	7.17	7.83
0.36	7.04	9.31	7.18	10.20	9.49	7.15	7.82
0.86	6.95	9.25	7.07	10.10	9.42	7.05	7.74
1.38	6.89	9.18	6.99	10.02	9.35	6.98	7.68
1.82	6.83	9.13	6.94	9.95	9.29	6.93	7.63
2.69	6.75	9.01	6.85	9.83	9.19	6.85	7.55
4.38	6.62	8.86	6.71	9.65	9.04	6.72	7.42
4.73	6.58	8.86	6.64	9.63	9.08	6.68	7.44
4.80	6.58	8.86	6.63	9.63	9.08	6.68	7.43
4.86	6.58	8.86	6.63	9.62	9.07	6.67	7.42

Table S5. Selected bond length (Å), bond angles (degree) and dihedral angles (degree) of COTh crystal at the S_0 (S_1) minimum and the modifications $\Delta|S_0-S_1|$ between the two states at different pressure (GPa).

Pressure	0			0.19			0.27			0.36			0.86			1.38			Exper. ⁷	
	S_0	S_1	$\Delta S_0-S_1 $	S_0	S_1	$\Delta S_0-S_1 $	S_0	S_1	$\Delta S_0-S_1 $	S_0	S_1	$\Delta S_0-S_1 $	S_0	S_1	$\Delta S_0-S_1 $	S_0	S_1	$\Delta S_0-S_1 $		
B₁	7-8	1.38	1.44	0.06	1.38	1.44	0.06	1.38	1.44	0.06	1.38	1.44	0.06	1.38	1.44	0.06	1.38	1.44	0.06	1.4
B₂	8-9	1.47	1.41	0.06	1.47	1.41	0.06	1.46	1.41	0.06	1.46	1.41	0.06	1.47	1.41	0.06	1.47	1.41	0.06	1.46
B₃	9-10	1.38	1.44	0.05	1.38	1.44	0.05	1.38	1.43	0.05	1.38	1.43	0.05	1.38	1.44	0.05	1.38	1.44	0.05	1.4
B₄	10-13	1.48	1.43	0.05	1.48	1.43	0.05	1.48	1.43	0.05	1.48	1.42	0.05	1.48	1.43	0.05	1.48	1.43	0.05	1.47
B₅	13-16	1.38	1.44	0.05	1.38	1.43	0.04	1.38	1.43	0.05	1.38	1.43	0.05	1.38	1.44	0.05	1.38	1.43	0.04	1.39
B₆	16-17	1.47	1.41	0.06	1.47	1.43	0.04	1.46	1.41	0.06	1.46	1.41	0.05	1.47	1.41	0.06	1.47	1.43	0.04	1.46
B₇	17-18	1.38	1.44	0.06	1.38	1.44	0.06	1.38	1.43	0.05	1.38	1.43	0.05	1.38	1.44	0.06	1.38	1.44	0.06	1.39
B₈	18-7	1.48	1.43	0.05	1.48	1.43	0.05	1.48	1.42	0.05	1.47	1.42	0.05	1.48	1.43	0.05	1.48	1.43	0.05	1.47
	7-8-9	129.5	129.2	0.3	129.5	129.1	0.3	129.4	129.0	0.5	129.2	128.7	0.5	129.5	129.2	0.3	129.5	129.1	0.3	129.9
	8-9-10	130.8	130.5	0.3	130.8	130.5	0.3	131.1	130.5	0.6	131.3	130.6	0.7	130.8	130.5	0.3	130.8	130.5	0.3	130.2
	8-7-18	126.1	126.9	0.8	126.1	126.8	0.7	126.2	126.7	0.4	126.3	126.5	0.2	126.1	126.9	0.8	126.1	126.8	0.7	125.8
	7-18-17	125.4	126.3	0.9	125.4	126.2	0.8	125.6	126.1	0.6	125.7	126.1	0.4	125.4	126.3	0.9	125.4	126.2	0.8	125.3
	18-7-8-9	5.4	6.9	1.4	5.7	7.0	1.3	6.4	7.4	1.0	7.3	7.9	0.6	5.4	6.9	1.4	5.7	7.0	1.3	2.0
	8-9-10-13	-1.2	-2.4	1.2	-1.5	-2.6	1.1	-1.9	-2.6	0.8	-2.4	-2.9	0.5	-1.2	-2.4	1.2	-1.5	-2.6	1.1	-0.3
	10-13-16-17	5.2	7.3	2.2	5.5	7.6	2.2	6.4	8.3	1.9	7.1	8.9	1.8	5.2	7.3	2.2	5.5	7.6	2.2	4.0
	16-17-18-7	0.0	-0.3	0.3	0.0	-0.3	0.3	0.0	-0.1	0.1	0.4	0.2	0.2	0.0	-0.3	0.3	0.0	-0.3	0.3	0.8
D₁	1-8-9-2	-48.4	-37.3	11.1	-48.3	-37.5	10.8	-47.9	-38.1	9.8	-47.8	-38.8	9.1	-48.4	-37.3	11.1	-48.3	-37.5	10.8	-47.2
D₂	11-10-13-14	45.3	35.3	9.9	45.4	35.7	9.7	45.6	36.6	8.9	46.5	37.9	8.6	45.3	35.3	9.9	45.4	35.7	9.7	44.0
D₃	4-16-17-3	-47.7	-37.6	10.1	-47.8	-38.0	9.7	-47.5	-39.0	8.5	-47.7	-40.0	7.7	-47.7	-37.6	10.1	-47.8	-38.0	9.7	-48.4
D₄	19-18-7-6	41.1	31.6	9.4	40.8	31.8	9.0	39.8	32.0	7.8	38.8	31.8	6.9	41.1	31.6	9.4	40.8	31.8	9.0	42.4

(continuous)

Table S5. Selected bond length (Å), bond angles (degree) and dihedral angles (degree) of COTh crystal at the S₀ (S₁) minimum and the modifications Δ|S₀-S₁| between the two states at different pressure (GPa).

Pressure		1.82			2.69			4.38			4.73			4.80			4.86		
		S ₀	S ₁	Δ S ₀ -S ₁	S ₀	S ₁	Δ S ₀ -S ₁	S ₀	S ₁	Δ S ₀ -S ₁	S ₀	S ₁	Δ S ₀ -S ₁	S ₀	S ₁	Δ S ₀ -S ₁	S ₀	S ₁	Δ S ₀ -S ₁
B₁	7-8	1.38	1.43	0.06	1.38	1.43	0.05	1.37	1.43	0.05									
B₂	8-9	1.46	1.41	0.06	1.46	1.40	0.05	1.45	1.39	0.05									
B₃	9-10	1.38	1.43	0.05															
B₄	10-13	1.48	1.42	0.05	1.47	1.42	0.05												
B₅	13-16	1.38	1.43	0.05	1.38	1.43	0.05	1.37	1.42	0.05									
B₆	16-17	1.46	1.41	0.05	1.46	1.40	0.05	1.45	1.40	0.05									
B₇	17-18	1.38	1.43	0.05	1.38	1.43	0.05	1.37	1.42	0.05									
B₈	18-7	1.47	1.42	0.05	1.47	1.42	0.05	1.46	1.41	0.05	1.46	1.41	0.05	1.45	1.41	0.05	1.45	1.41	0.05
	7-8-9	129.1	128.5	0.6	128.7	128.0	0.7	128.0	127.3	0.7	128.4	127.7	0.7	128.4	127.6	0.7	128.3	127.6	0.7
	8-9-10	131.5	130.7	0.8	131.9	131.0	0.9	132.6	131.6	1.0	132.7	131.7	1.0	132.8	131.8	1.0	132.8	131.8	1.0
	8-7-18	126.3	126.4	0.1	126.4	126.3	0.1	126.6	126.3	0.4	126.9	126.5	0.4	126.9	126.5	0.4	126.9	126.4	0.4
	7-18-17	125.9	126.2	0.3	126.1	126.2	0.1	126.6	126.6	0.0	126.9	126.9	0.0	126.9	126.9	0.0	127.0	127.0	0.0
	18-7-8-9	8.1	8.4	0.3	9.7	9.7	0.0	12.2	11.7	0.5	11.5	11.1	0.4	11.6	11.1	0.5	11.7	11.2	0.5
	8-9-10-13	-2.8	-3.0	0.2	-4.0	-3.8	0.2	-5.5	-4.6	0.9	-6.4	-5.3	1.1	-6.3	-5.1	1.1	-6.1	-5.0	1.1
	10-13-16-17	7.7	9.5	1.8	9.1	10.9	1.8	10.9	12.7	1.8	11.0	12.8	1.8	11.0	12.8	1.8	11.0	12.8	1.8
	16-17-18-7	0.7	0.5	0.2	1.2	0.9	0.3	3.0	2.4	0.6	3.8	3.3	0.6	4.0	3.4	0.5	4.2	3.6	0.5
D₁	1-8-9-2	-47.8	-39.2	8.6	-47.9	-39.8	8.0	-47.9	-40.9	7.0	-46.4	-39.6	6.8	-46.5	-39.7	6.8	-46.5	-39.7	6.8
D₂	11-10-13-14	47.2	38.9	8.3	49.1	41.0	8.2	52.7	44.7	8.0	53.0	45.1	7.9	53.0	45.2	7.8	53.1	45.2	7.8
D₃	4-16-17-3	-47.8	-40.5	7.3	-48.5	-41.8	6.7	-49.2	-43.1	6.1	-49.4	-43.3	6.0	-49.3	-43.3	6.0	-49.3	-43.3	6.0
D₄	19-18-7-6	37.9	31.5	6.4	36.3	30.9	5.5	33.0	28.4	4.6	32.4	28.0	4.4	32.2	27.9	4.4	32.1	27.7	-4.4

Table S6. The calculated vertical excitation energy (ΔE_{vert}), oscillator strength (f), adiabatic excitation energy (ΔE_{ad}) and the transition orbital assignment for S_1 of COTh molecules at crystal state under different pressure.

Pressure (GPa)	ΔE_{vert} (eV)	f	ΔE_{ad} (eV)	Transition orbital assignment
0	2.313	0.0038	2.858	HOMO→LUMO 99.18%
0.19	2.350	0.0039	2.884	HOMO→LUMO 99.15%
0.27	2.357	0.0040	2.887	HOMO→LUMO 99.15%
0.36	2.372	0.0041	2.898	HOMO→LUMO 99.13%
0.86	2.411	0.0042	2.924	HOMO→LUMO 99.11%
1.38	2.451	0.0044	2.951	HOMO→LUMO 99.08%
1.82	2.479	0.0045	2.970	HOMO→LUMO 99.05%
2.69	2.534	0.0049	3.007	HOMO→LUMO 99.00%
4.38	2.615	0.0058	3.052	HOMO→LUMO 98.88%
4.73	2.604	0.0063	3.039	HOMO→LUMO 98.84%
4.80	2.606	0.0063	3.039	HOMO→LUMO 98.84%
4.86	2.610	0.0063	3.041	HOMO→LUMO 98.84%

Table S7. The calculated spin-orbit coupling constants between S_1 and triplet excited states for COTh crystals at 0 GPa and 4.86 GPa.

Pressure (GPa)	SOC (cm^{-1})
0	1.1
4.86	1.4

Table S8. The calculated k_r , k_{ic} , k_{eet} and fluorescence quantum efficiency Φ_F for the COTh aggregates under different pressure.

Pressure (GPa)	$k_r(10^6 \text{ s}^{-1})$	$k_{ic}(10^6 \text{ s}^{-1})$	$k_{eet}(10^6 \text{ s}^{-1})$	Φ_F
0	0.882	29.65	20.04	1.74%
0.19	0.934	18.07	38.48	1.63%
0.27	0.964	15.82	52.23	1.40%
0.36	1.002	12.86	66.34	1.25%
0.86	1.060	8.001	157.2	0.64%
1.38	1.147	5.673	293.6	0.38%
1.82	1.200	5.037	518.3	0.23%
2.69	1.366	8.846	1669	0.08%
4.38	1.721	9.613	2630	0.07%
4.73	1.854	2.114	1527	0.12%
4.80	1.857	1.996	1580	0.12%
4.86	1.862	1.932	1607	0.12%

Table S9. The calculated λ_{gs} , λ_{es} and λ_{total} of COTh in aggregates at different pressures.

Pressure (GPa)	λ_{gs} (meV)	λ_{es} (meV)	λ_{total} (meV)
0	639	650	1289
0.19	619	618	1237
0.27	612	606	1218
0.36	604	594	1197
0.86	577	557	1134
1.38	559	532	1090
1.82	546	516	1062
2.69	528	495	1023
4.38	502	464	966
4.73	499	462	961
4.80	498	461	959
4.86	496	459	955

Table S10. The maximum J_{\max} among different dimers and spectral overlap I under different pressure for COTh crystals.

Pressure (GPa)	J_{\max} (meV)	I (meV $^{-1}$)
0	1.894	0.585
0.19	1.963	1.050
0.27	1.994	1.380
0.36	2.006	1.730
0.86	2.069	3.850
1.38	2.118	6.860
1.82	2.174	11.490
2.69	2.418	29.890
4.38	2.772	33.880
4.73	2.981	17.990
4.80	2.985	18.580
4.86	2.960	19.210

Table S11. The transfer integral V (meV) along different pathways under different pressure.

Pressure (GPa)	1,1'	2,2'	3,3'	4,4'	5,5'	6,6'	7,7'
0	41.1	19.2	2.0	1.1	6.0	6.5	2.1
0.19	43.4	20.6	1.0	1.3	6.4	7.2	2.8
0.27	40.2	21.0	0.2	1.3	6.3	7.3	3.9
0.36	42.4	21.8	0.4	1.4	6.4	7.8	3.8
0.86	45.5	24.1	3.4	1.4	7.2	9.7	4.8
1.38	49.3	26.4	5.1	1.5	7.5	11.2	6.1
1.82	52.1	28.2	6.6	1.6	7.8	12.6	7.0
2.69	59.8	31.8	8.6	1.8	7.8	14.9	8.4
4.38	69.9	37.5	12.0	2.1	7.4	19.0	11.5
4.73	70.3	39.7	15.7	1.8	7.3	21.5	10.6
4.80	70.1	39.8	15.9	1.8	7.4	21.8	10.9
4.86	70.4	39.9	16.0	1.8	7.5	22.0	11.2

Table S12. The calculated charge reorganization energy λ_{charge} using normal mode analysis (NM) and adiabatic potential energy surface method (AP) at different pressure.

Pressure	λ_{charge}	
	AP	NM
0	314	330
0.19	306	320
0.27	302	315
0.36	298	310
0.86	287	298
1.38	280	290
1.82	275	284
2.69	267	276
4.38	257	265
4.73	256	266
4.80	256	265
4.86	256	264

Reference

1. G. Nan, X. Yang, L. Wang, Z. Shuai and Y. Zhao, *Phys. Rev. B*, 2009, **79**, 115203.
2. M. Malagoli and J. L. Brédas, *Chem. Phys. Lett.*, 2000, **327**, 13-17.
3. V. Lemaur, D. A. da Silva Filho, V. Coropceanu, M. Lehmann, Y. Geerts, J. Piris, M. G. Debije, A. M. van de Craats, K. Senthilkumar, L. D. A. Siebbeles, J. M. Warman, J.-L. Brédas and J. Cornil, *J. Am. Chem. Soc.*, 2004, **126**, 3271-3279.
4. O. Kwon, V. Coropceanu, N. E. Gruhn, J. C. Durivage, J. G. Laquindanum, H. E. Katz, J. Cornil and J. L. Brédas, *J. Chem. Phys.*, 2004, **120**, 8186-8194.
5. R. S. Sánchez-Carrera, V. Coropceanu, D. A. da Silva Filho, R. Friedlein, W. Osikowicz, R. Murdey, C. Suess, W. R. Salaneck and J.-L. Brédas, *J. Phys. Chem. B*, 2006, **110**, 18904-18911.
6. E. F. Valeev, V. Coropceanu, D. A. da Silva Filho, S. Salman and J.-L. Brédas, *J. Am. Chem. Soc.*, 2006, **128**, 9882-9886.
7. Z. Zhao, X. Zheng, L. Du, Y. Xiong, W. He, X. Gao, C. Li, Y. Liu, B. Xu, J. Zhang, F. Song, Y. Yu, X. Zhao, Y. Cai, X. He, R. T. K. Kwok, J. W. Y. Lam, X. Huang, D. Lee Phillips, H. Wang and B. Z. Tang, *Nat. Commun.*, 2019, **10**, 2952.